ChemComm

COMMUNICATION

Facile synthesis of silicon nanoparticles inserted into graphene sheets as improved anode materials for lithium-ion batteries†

Xiaosi Zhou, Ya-Xia Yin, Li-Jun Wan and Yu-Guo Guo*

Silicon nanoparticles have been successfully inserted into graphene sheets *via* a novel method combining freeze-drying and thermal reduction. The as-obtained Si/graphene nanocomposite exhibits remarkably enhanced cycling performance and rate performance compared with bare Si nanoparticles for lithium-ion batteries.

The development of high energy density and long cycle life lithium-ion batteries is of great technological importance for use in portable electronics, electric vehicles, and the storage of renewable energy.[1–6] To meet these requirements, the electrode materials of lithium-ion batteries must have high specific storage capacities and satisfactory cycle life. Recently, silicon has been intensively investigated for use as high-capacity anode material owing to its highest known capacity (4200 mA h g^{-1}), which is ten times higher than that of graphite (372 mA h g^{-1}).[7–11] Unfortunately, the practical application of silicon as an anode material is seriously hindered by the huge volume changes (>300%) and low intrinsic electrical conductivity during lithium uptake and release from silicon, leading to dramatic pulverization of silicon nanoparticles and rapid capacity fading.[12,13] To overcome these issues and improve the overall electrochemical performance of silicon anodes, one effective strategy is to use carbon coatings, which can not only restrict the large volume change of silicon to keep the electrode integrity, but also enhance the electrical conductivity. For example, Liu and co-workers reported carbon-coated silicon nanocomposites with high capacities prepared by a spray-pyrolysis technique.[14] Hu *et al.* synthesized $Si@SiO_x/C$ nanocomposites with good electrochemical performance by a hydrothermal carbonization method.[12] Another effective strategy is to fabricate silicon nanostructures, such as nanowires, nanotubes, and nanospheres, in which the stress caused by the volume change can be accommodated more easily than that in bulk silicon.[13] Recently, Yushin *et al.* have reported nanosized Si-in-C tubes which were fabricated using chemical vapor deposition (CVD) and exhibited high capacity and stable performance.[15] Cui and Yao *et al.* have prepared interconnected silicon hollow nanospheres by CVD

and a template etching method and achieved a high initial discharge capacity of 2725 mA h g^{-1} with excellent cycling performance.[16] More recently, our group have reported $Cu@Si@Al_2O_3$ nanocable arrays and silicon/carbon nanoporous microspheres with favorable cycling and rate performance.[17,18] So far, advanced carbon coatings for silicon-based nanomaterials and their facile fabrication methods are still highly desired toward cost-effective anode materials.

Graphene, a two-dimensional carbon nanomaterial, has attracted enormous attention owing to its unique properties and potential applications in the areas of electronics as well as energy conversion and storage devices.[19–23] Recently, it has been demonstrated that graphene is very useful in the design of superior anode materials for lithium-ion batteries due to its high electronic conductivity, mechanical strength, and flexibility.[24] However, in the cases of silicon-based anode materials, there are still many difficulties in the utilization of graphene. For example, silicon nanoparticles are difficult to be homogeneously dispersed within graphene layers by simply mechanical blending.[25] High temperature commonly used during the synthesis of graphene/nanosized silicon composites often leads to the conglomeration of silicon nanoparticles.[26] In addition, the electrode films obtained from the assembly of silicon nanoparticles and graphene by filtration might be too thick to guarantee quick lithium ion diffusion into the structure.[27,28] An advanced technique for inserting Si nanoparticles into graphene sheets remains a great challenge. Herein, we report a facile method for preparing such structures. Silicon nanoparticles inserted uniformly into graphene are realized by combining freeze-drying and thermal reduction. The as-prepared silicon nanoparticles intercalated in graphene sheets form a typical hierarchical micro–nano structure, in which graphene plays the roles of both an electronically conductive network and an elastic buffer for the silicon nanoparticles. As a result the cycling performance and rate capability of the silicon nanoparticles inserted into graphene are significantly improved when being used as anode materials in lithium-ion batteries.
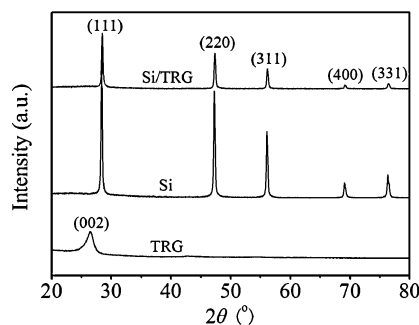
Freeze-drying is defined as direct sublimation of solvents under vacuum to dry samples and maintain their microstructures. It is a well-established approach to create aligned porous structures,[29] three-dimensional nanocomposites,[30] and organic nanoparticles.[31] Graphite oxide (GO) obtained from the modified Hummer method was used as the precursor of graphene sheets and silicon nanoparticles (<300 nm) were used as starting materials

Institute of Chemistry, Chinese Academy of Sciences (CAS), Beijing 100190, P. R. China. E-mail: ygguo@iccas.ac.cn; Fax: +86-10-62557908
† Electronic supplementary information (ESI) available: Experimental section, additional data on Si/TRG composites and Si nanoparticles. See DOI: 10.1039/c2cc17061b
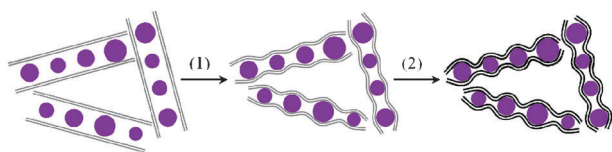
Fig. 1 Schematic illustration of the synthesis route for silicon nanoparticles inserted into graphene. Grey lines (graphene oxide), black lines (thermally reduced graphene), and purple balls (silicon nanoparticles). (1) Freeze-drying, and (2) thermal reduction.

Fig. 2 XRD patterns of the Si/TRG composites, Si nanoparticles, and TRG.

Fig. 3 SEM images (a and b) and TEM images (c and d) of the Si/TRG composites.

(see Fig. S1 and S2 in the ESI†).[32] The approach to the synthesis of silicon/thermally reduced graphene (Si/TRG) composites is schematically illustrated in Fig. 1 (the details of the synthesis are described in ESI†). Typically, the aqueous mixture of graphene oxide and silicon nanoparticles was freeze-dried, followed by thermal reduction of the as-freeze-dried mixture at 700 °C to obtain the Si/TRG composites. Fig. 2 shows the X-ray diffraction (XRD) patterns of the Si/TRG composites, Si nanoparticles, and TRG. The pattern of Si/TRG composites is the same as that of pure Si nanoparticles, implying that the silicon crystals in the Si/TRG composites are not destroyed during the freeze-drying and thermal reduction processes. In the XRD pattern of the TRG sample obtained with the same procedure of Si/TRG, the characteristic peak (2θ) appears at 26.4°, corresponding to a layer-to-layer distance (d-spacing) of 0.338 nm, which is close to the d-spacing ($ca.$ 0.335 nm) of natural graphite.[33] The result confirms the well-packed layered structure of TRG. This characteristic peak is indistinctive in the pattern of Si/TRG, which might be attributed to the dispersion of graphene sheets by Si nanoparticles. Moreover, the X-ray photoelectron spectroscopy (XPS) survey confirms that the silicon particles are covered with graphene and the oxygen functionalities of GO are severely decreased during the thermal reduction process (Fig. S3, ESI†).

To verify the morphology, structure and composition of the Si/TRG composites, we carried out the scanning electron microscopy (SEM), transmission electron microscopy (TEM), and energy dispersive X-ray spectroscopy (EDX, Fig. S4, ESI†) analysis of the material. The SEM images show that the Si/TRG composites are micrometre-sized aggregates with few exposed Si nanoparticles on the surface (Fig. 3a and b). The TEM images reveal that the micrometre-sized aggregates are made from Si nanoparticles and graphene sheets (Fig. 3c and Fig. S5 in ESI†). The typically wrinkled graphene sheets form a network and well cover the highly dispersed Si nanoparticles. The HRTEM images reveal that a single 20 nm Si nanocrystal

intercalates in graphene sheets with a thickness less than 2 nm, and nanospace exists between the Si nanocrystal and graphene sheets (Fig. 3d and Fig. S6 in ESI†). The EDX analysis shows that the Si/TRG composites are composed of Si, C, and O. The thermal gravimetric analysis (TGA) reveals that the Si/TRG composites contain 82.1 wt% of Si and 17.9 wt% of graphene (Fig. S7 in ESI†). Moreover, a low Brunauer–Emmett–Teller (BET) surface area of 85 m² g⁻¹ is measured for the composite. The nitrogen adsorption–desorption isotherm represents a typical IV-type isotherm with an associated H3 type hysteresis loop, indicating the mesoporous structure of the Si/TRG composite, which is further confirmed by the Barrett–Joyner–Halenda (BJH) pore-size distribution (Fig. S8 in ESI†). In short, the above results suggest that the Si/TRG composites are composed of Si nanoparticles and graphene, the Si nanoparticles insert into graphene, and nanospace exists between the Si nanoparticles and graphene sheets. The unique structure is expected for superior lithium storage because it facilitates the conduction of electrons and the diffusion of lithium ions and provides elastic buffer to accommodate the volume variation of Si nanoparticles during Li alloying and dealloying processes.

Fig. 4a shows the first three cyclic voltammetry (CV) curves of the Si/TRG composites in the potential window of 0.05–1 V at a scan rate of 0.1 mV s⁻¹. In the first cycle a broad cathodic peak appeared at 0.78 V resulting from the formation of solid electrolyte interphase (SEI), and leads to an initial irreversible capacity.[34] The cathodic sweep of the second CV curve displays two peaks at 0.051 and 0.20 V, corresponding to the formation of Li–Si alloy phases, while the two peaks at 0.31 and 0.50 V at the anodic sweep could be ascribed to dealloying of Li–Si alloys (Scheme S1 in ESI†). The results are well consistent with the data reported in the literature.[35]

Fig. 4b displays the discharge–charge profiles of the Si/TRG composites cycled at a current density of 200 mA g⁻¹ between the voltage limits of 0.05–1 V $vs.$ Li⁺/Li. The initial discharge capacity is 3070 mA h g⁻¹ with a reversible charge capacity up to 1866 mA h g⁻¹. Note that the specific capacity is based on

Fig. 4 (a) Cyclic voltammetry profiles of the Si/TRG composites and (b) galvanostatic discharge–charge curves for different cycles. (c) Cycling performance of the Si/TRG composites and Si nanoparticles. (d) Rate capability of the Si/TRG composites.

the total mass of the Si/TRG composites in the context. After the first cycle, the Coulombic efficiency could increase and stabilize at 98%–100% in subsequent cycles. For comparison, pristine Si nanoparticles were also tested for lithium-ion batteries. Apparently, the Si/TRG composites show much better cycling performance than the Si nanoparticles (Fig. 4c). After 100 cycles, the reversible capacity of Si/TRG composites is still as high as 1153 mA h g^{-1}, which is more than 3 times higher than that of the theoretical specific capacity of currently used graphite (LiC$_6$, 372 mA h g^{-1}), while that of Si nanoparticles is only 13 mA h g^{-1}. Another much improved property of the Si/TRG composites is their excellent rate capability (Fig. 4d). The Si/TRG composites exhibit stable and reversible capacities of 1304, 1014, and 803 mA h g^{-1} when the current densities increase from 1000 mA g^{-1}, to 2000 mA g^{-1}, and 4000 mA g^{-1}. The superior cycling and rate performances of Si/TRG composites could be attributed to the following reasons. On the one hand, the graphene sheets could provide sufficient electrons for the Si nanoparticles, withstand the deformation pressure from Li–Si alloying and dealloying processes, and maintain an integrated structure. On the other hand, the existence of nanospace between graphene sheets and Si nanoparticles could enhance Li$^+$ diffusion to the encapsulated Si nanoparticles, as well as accommodate the alloyed Si nanoparticles. Electrochemical impedance spectroscopy (EIS) measurements of the samples before and after being used clearly indicate the enhanced electronic conductivity and less SEI formation for the Si/TRG composites compared to pristine Si nanoparticles (Fig. S9 in ESI†). The robust structure of the Si/TRG composites is confirmed by the TEM images of the sample after being used in lithium-ion batteries for 100 cycles (see Fig. S10 in ESI†).

In summary, we have developed a novel method for the preparation of Si nanoparticles intercalated in graphene sheets *via* combining freeze-drying and thermal reduction. The as-achieved Si/TRG composites exhibit remarkably improved cycling performance (*ca.* 1153 mA h g^{-1} after 100 cycles) and rate performance in comparison with bare Si nanoparticles, which could be attributed to the unique structure of the nanocomposite. In addition, the obtained nanocomposites are micrometre-sized aggregates which

promise ease of process. Taking the facile synthesis and excellent performance of Si/TRG composites into account, it would be of significant interest to extend to other high capacity electrode materials with large volume change and low electronic conductivity.

Notes and references

1 J. Maier, *Nat. Mater.*, 2005, **4**, 805.
2 A. S. Aricò, P. Bruce, B. Scrosati, J.-M. Tarascon and W. V. Schalkwijk, *Nat. Mater.*, 2005, **4**, 366.
3 M. Armand and J.-M. Tarascon, *Nature*, 2008, **451**, 652.
4 X. Ji, K. T. Lee and L. F. Nazar, *Nat. Mater.*, 2009, **8**, 500.
5 Y.-G. Guo, J.-S. Hu and L.-J. Wan, *Adv. Mater.*, 2008, **20**, 2878.
6 X. L. Wu, L. Y. Jiang, F. F. Cao, Y.-G. Guo and L.-J. Wan, *Adv. Mater.*, 2009, **21**, 2710.
7 C. K. Chan, H. Peng, G. Liu, K. Mcilwrath, X. F. Zhang, R. A. Huggins and Y. Cui, *Nat. Nanotechnol.*, 2007, **3**, 31.
8 H. Li, X. Huang, L. Chen, Z. Wu and Y. Liang, *Electrochem. Solid-State Lett.*, 1999, **2**, 547.
9 H. Ma, F. Cheng, J. Chen, J. Zhao, C. Li, Z. Tao and J. Liang, *Adv. Mater.*, 2007, **19**, 4067.
10 H.-Y. Lee and S.-M. Lee, *Electrochem. Commun.*, 2004, **6**, 465.
11 H. K. Liu, Z. P. Guo, J. Z. Wang and K. Konstantinov, *J. Mater. Chem.*, 2010, **20**, 10055.
12 Y.-S. Hu, R. Demir-Cakan, M.-M. Titirici, J.-O. Müller, R. Schlögl, M. Antonietti and J. Maier, *Angew. Chem., Int. Ed.*, 2008, **47**, 1645.
13 Y. Hu, L. Gu, C. Zhu, S. Tsukimoto, P. A. van Aken and J. Maier, *Adv. Mater.*, 2010, **22**, 2247.
14 S.-H. Ng, J. Wang, D. Wexler, K. Konstantinov, Z.-P. Guo and H.-K. Liu, *Angew. Chem., Int. Ed.*, 2006, **45**, 6896.
15 B. Hertzberg, A. ALexeev and G. Yushin, *J. Am. Chem. Soc.*, 2010, **132**, 8548.
16 Y. Yao, M. T. McDowell, I. Ryu, H. Wu, N. Liu, L. Hu, W. D. Nix and Y. Cui, *Nano Lett.*, 2011, **11**, 2949.
17 F.-F. Cao, J.-W. Deng, S. Xin, H.-X. Ji, O. G. Schmidt, L.-J. Wan and Y.-G. Guo, *Adv. Mater.*, 2011, **23**, 4415.
18 Y.-X. Yin, S. Xin, L.-J. Wan, C.-J. Li and Y.-G. Guo, *J. Phys. Chem. C*, 2011, **115**, 14148.
19 K. S. Novoseolov, A. K. Geim, S. V. Morozov, D. Jiang, Y. Zhang, S. V. Dubonos, I. V. Grigorieva and A. A. Firsov, *Science*, 2004, **306**, 666.
20 X. Zhou, T. Wu, B. Hu, G. Yang and B. Han, *Chem. Commun.*, 2010, **46**, 3663.
21 H. Wang, Y. Yang, Y. Liang, J. T. Robinson, Y. Li, A. Jackson, Y. Cui and H. Dai, *Nano Lett.*, 2011, **11**, 2644.
22 X.-L. Wang and W.-Q. Han, *ACS Appl. Mater. Interfaces*, 2010, **2**, 3709.
23 H. Jia, P. Gao, J. Yang, J. Wang, Y. Nuli and Z. Yang, *Adv. Energy Mater.*, 2011, **1**, 1036.
24 S. Yang, X. Feng, L. Wang, K. Tang, J. Maier and K. Müllen, *Angew. Chem., Int. Ed.*, 2010, **49**, 4795.
25 S.-L. Chou, J.-Z. Wang, M. Choucair, H.-K. Liu, J. A. Stride and S.-X. Dou, *Electrochem. Commun.*, 2010, **12**, 303.
26 H. Xiang, K. Zhang, G. Ji, J. Y. Lee, C. Zou, X. Chen and J. Wu, *Carbon*, 2011, **49**, 1787.
27 J. K. Lee, K. B. Smith, C. M. Hayner and H. H. Kung, *Chem. Commun.*, 2010, **46**, 2025.
28 J.-Z. Wang, C. Zhong, S.-L. Chou and H.-K. Liu, *Electrochem. Commun.*, 2010, **12**, 1467.
29 H. Zhang, I. Hussain, M. Brust, M. F. Butler, S. P. Rannard and A. I. Cooper, *Nat. Mater.*, 2005, **4**, 787.
30 J. L. Vickery, A. J. Patil and S. Mann, *Adv. Mater.*, 2009, **21**, 2180.
31 L. Qian, A. Ahmed and H. Zhang, *Chem. Commun.*, 2011, **47**, 10001.
32 W. S. Hummers and R. E. Offeman, *J. Am. Chem. Soc.*, 1958, **80**, 1339.
33 A. R. Landgebe and Z.-I. Takehara, *Proceeding of the Symposium on Batteries and Fuel Cells for Stationary and Electric Vehical Applications*, The Electrochemical Society, 1993, p. 66.
34 P. Liu and H. Wu, *J. Power Sources*, 1995, **56**, 81.
35 J. Li and J. R. Dahn, *J. Electrochem. Soc.*, 2007, **154**, A156.